Supporting Information

β-cyclodextrin coated SiO_2@Au@Ag core/shell nanoparticles for SERS detection of PCBs

Yilin Lu[a], Guohua Yao[a], Kexi Sun[a] and Qing Huang*[ab]

[a.] *Key Laboratory of Ion Beam Bioengineering, Institute of Technical Biology and Agriculture Engineering, Hefei Institutes of Physical Science, Chinese Academy of Sciences, China*

[b.] *University of Science & Technology of China, Hefei, Anhui 230026, PR China*

Contact information：

P.O. Box 1138, Shushanhu Road 350, Hefei 230031, PR China

*Corresponding Authors: Prof. Dr. Qing Huang

Address: P. O. Box 1138, Hefei 230031, P. R. China

Phone Number: 86-551-65595261

Fax Number: 86-551-65595261

E-mail Address: huangq@ipp.ac.cn

The Supporting Information includes:

Part S1. Measurement of zeta (ζ) potential

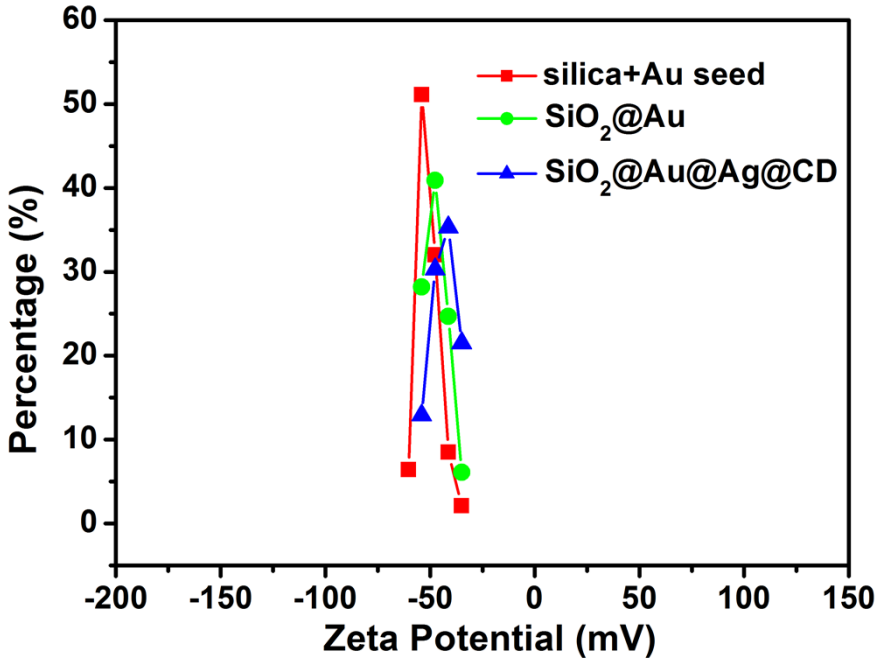

Fig. S1 Zeta potentials for the fabricated silica+Au seeds, SiO_2@Au NPs and SiO_2@Au@Ag@CD NPs.

Part S2. SEM pictures of the SiO_2@Au@Ag@CD NPs

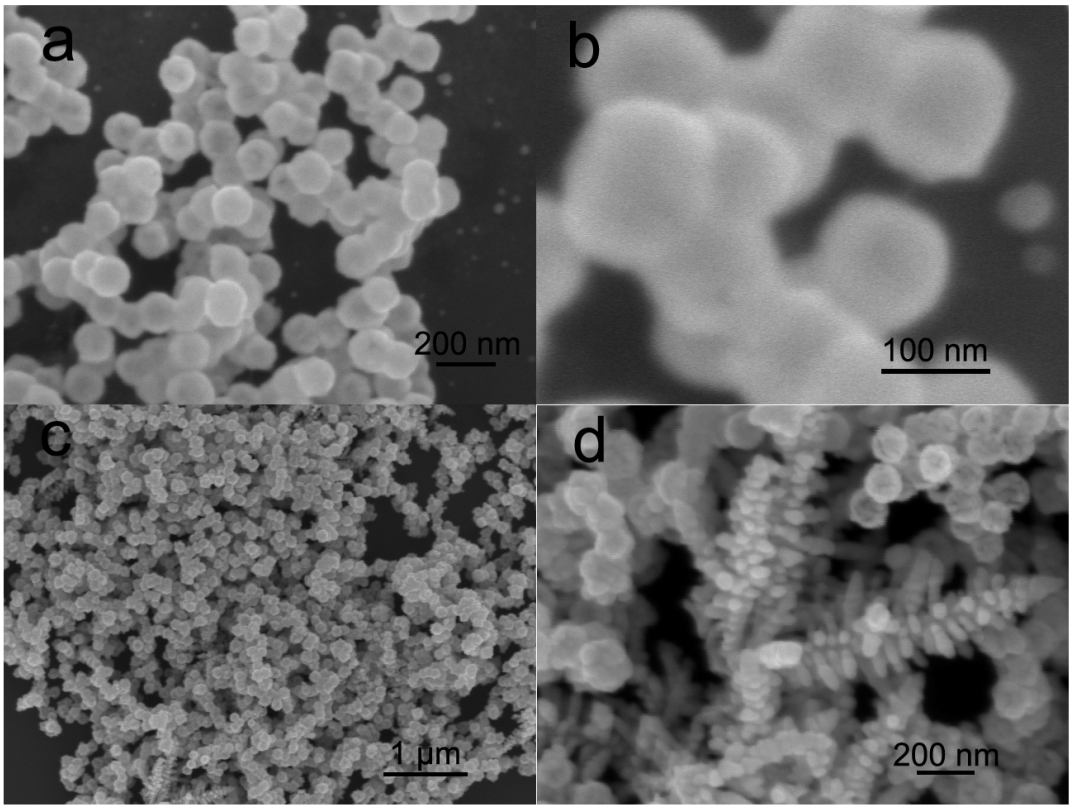

Fig. S2 SEM images of the SiO_2@Au@Ag@CD NPs obtained at different contents of $AgNO_3$: (a) 250 μL and (c) 400 μL, while the images (b) and (d) are the high resolution SEM images of (a) and (c), respectively.

Part S3. EDS analysis of SiO_2@Au and SiO_2@Au@Ag@CD NPs

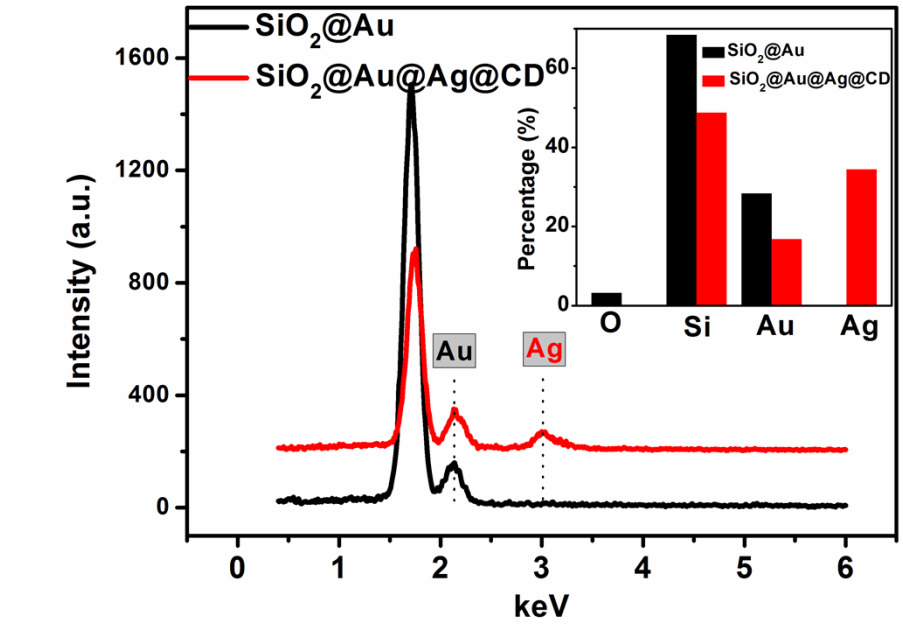

Fig.S3 EDS spectra of the fabricated SiO_2@Au and SiO_2@Au@Ag@CD NPs

Part S4. FT-IR measurements of β-CD, SiO_2@Au and SiO_2@Au@Ag@CD NPs

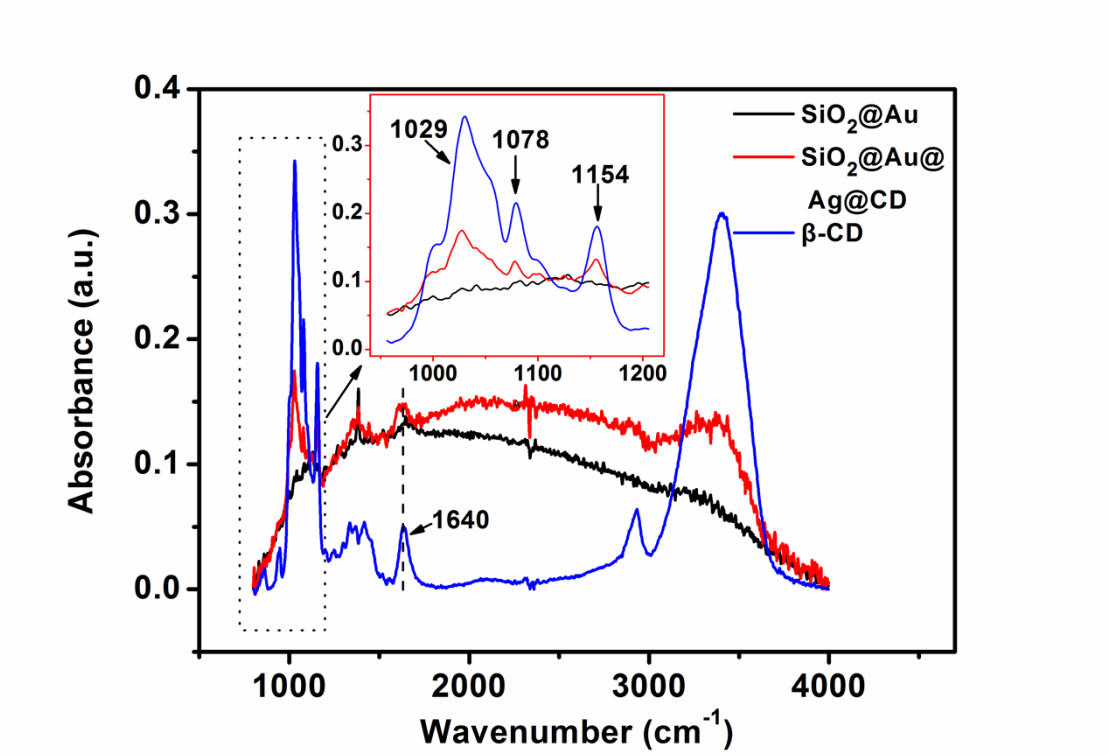

Fig. S4 FT-IR spectra of β-CD, SiO_2@Au and SiO_2@Au@Ag@CD NPs, respectively. The inset plot is magnification of the spectra in the range from 900 to 1200 cm^{-1}.

Table. S1 The assignments of the most intense bands of β-CD.[1-2]

Wavenumber(cm^{-1})	Vibrational mode assignment
3390	O-H stretch
1640	O-H bending
1356	O-H deformation
1154	C-O stretching
1078	CO/CC stretching
1029	CO/CC stretching

Part S5. SEM pictures of Ag@CD and SiO_2@Ag@CD NPs

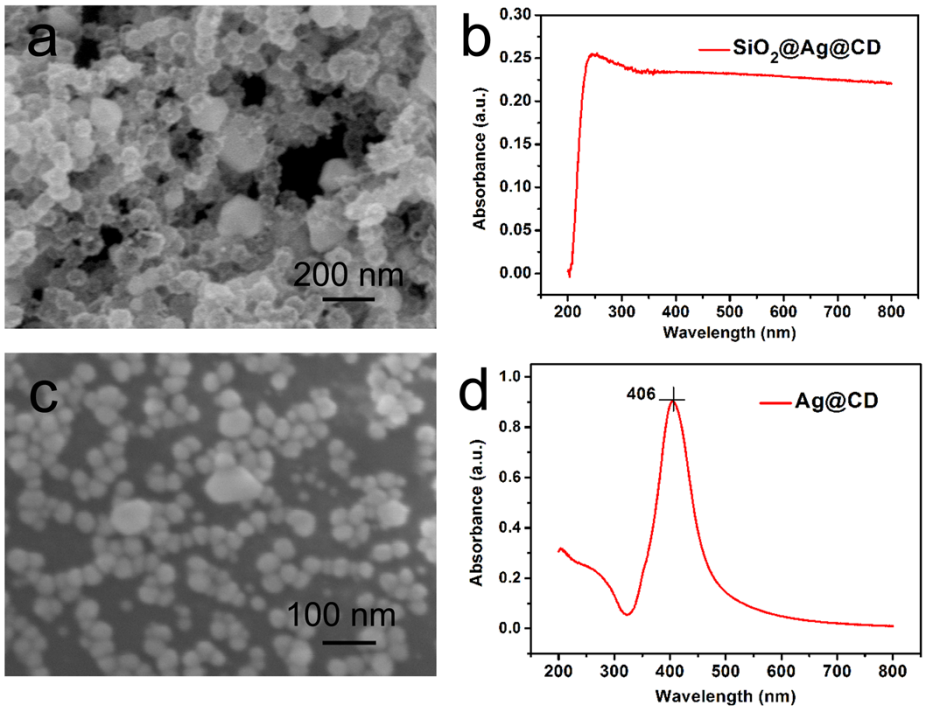

Fig.S5 (a) SEM picture of the products of silica-Au seeds reacted with β-CD. The synthesis route is similar to that for the SiO_2@Au@Ag@CD NPs except skipping the Au shell formation step. (b) UV-vis spectra of the SiO_2@Ag@CD NPs in water solution. (c) SEM picture of the Ag NPs synthesized by reduction of β-cyclodextrin directly, denoted as Ag@CD NPs. (d) UV-vis spectra of the Ag@CD NPs.

Part S6. Calculation of enhancement factor (EF)

The SERS signals of R6G measured on the SiO_2@Au@Ag@CD substrate were compared with the intensities of the normal Raman signals of R6G so that the SERS enhancement factor (EF) can be estimated according to the following equation given by the literature[3]:

$$EF = \frac{I_{SERS} / N_{SERS}}{I_{RS} / N_{RS}} \quad (1)$$

where the intensity I_{SERS} and I_{RS} correspond to the Raman signal recorded from the SERS substrate and from the sample spread on a silicon wafer, respectively, and N_{SERS} and N_{RS} refer to the amount of R6G molecules localized in the illumination volume of the laser focus spot on the SERS substrate and on the silicon wafer, respectively. Since the measuring conditions such as laser wavelength, laser power, and recording time are identical, the above equation can be rewritten as:

$$EF = \frac{I_{SERS}}{I_{RS}} \bullet \frac{S_{SERS} V_{RS} C_{RS}}{S_{RS} V_{SERS} C_{SERS}} \quad (2)$$

In the SERS measurement, 8 μL of 10^{-10} M R6G solution was added to the surface of the substrate containing SiO_2@Au@Ag@CD NPs. The area of solution was about 24 mm^2 after the evaporation of ethanol. For the normal Raman measurement, 10 μL of 10^{-3} M R6G solution was dripped and spread on the silicon wafer, and the area of solution was about 9 mm^2. The intensity of the C-C-C ring in-plane vibration mode of R6G at 612 cm^{-1} band was used to estimate the EF value, and the I_{SERS} and I_{RS} are 1071 and 1589 (arbitrary unit), respectively. Substituting these recorded values into the above equation, the EF was evaluated to be 2.247×10^7.

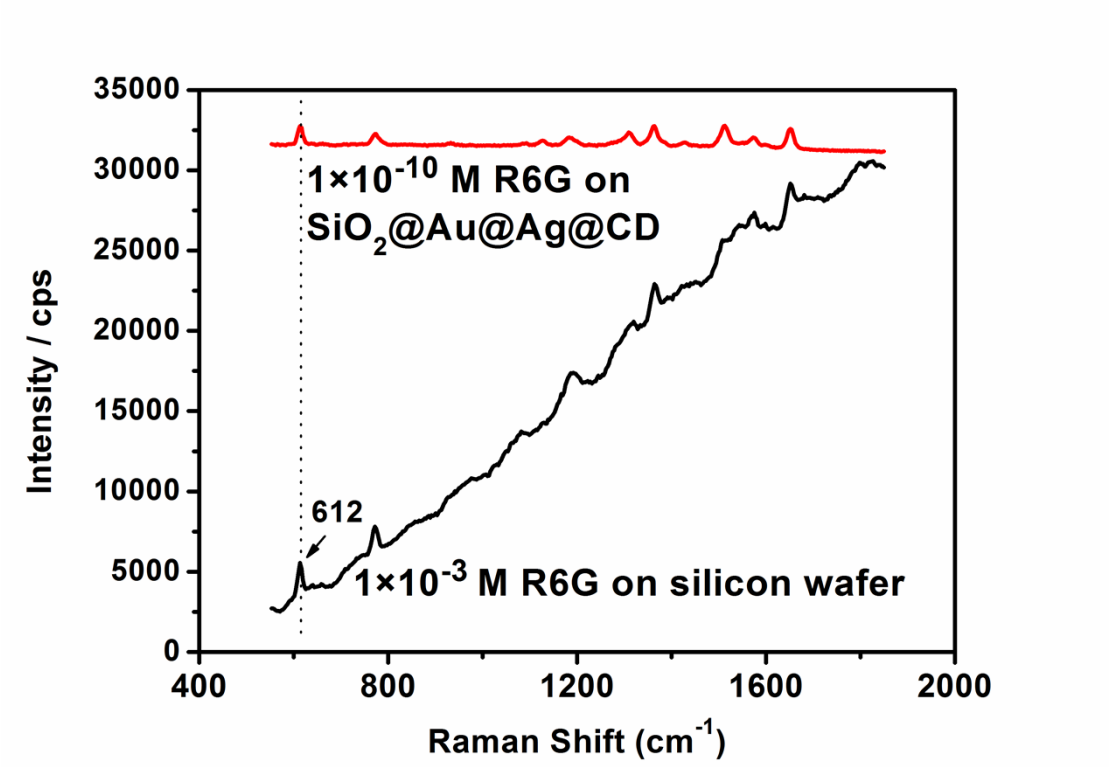

Fig. S6 Raman spectrum of 1×10^{-3} M R6G aqueous solution spread on the silicon wafer (below) and SERS spectrum of 1×10^{-10} M R6G adsorbed on the SiO_2@Au@Ag@CD substrate (above). (cps: counts per second).

Table. S2 The assignments of the Raman bands in SERS spectra of R6G.[4-5]

Frequency (cm^{-1})	Assignment
612	C-C-C ring in-plane bending
773	out-of-plane bending
1192	C-C stretching vibrations
1362	aromatic C-C stretching vibrations
1513	aromatic C-C stretching vibrations
1652	aromatic C-C stretching vibrations

Part S7. Finite element method (FEM) modeling of the core/shell nanoparticles

In order to get a better understanding the Raman enhancement for the growth of the Ag layer, FEM modeling was employed to investigate the change of the localized electromagnetic field intensity of SiO_2@Au and SiO_2@Au@Ag NPs with the changes of their gaps. The FEM modeling was performed using Comsol Multiphysics V3.5a, and the optical constants of Ag(ε_{Ag}=-11.84+0.45*i*), Au(ε_{Au}= -4.6+2.5*i*) and silica(ε=2.136) at wavelength of 532 nm were taken from the literatures[6-7].

The SiO_2@Au@Ag NPs were recognized as core-shell spherical structure with diameter about 140 nm as obtained from the SEM observation, with the corresponding thickness of Au layer and Ag layer was about 10 nm and 10 nm, respectively. For comparison, the size of SiO_2@Au NPs applied is same as that of SiO_2@Au@Ag NPs expect for the additional Ag layer. And the diameter of SiO_2@Ag NPs is 140 nm with the diameter of silica about 100 nm. Our calculation confirms that the induction of the Ag layer can significantly improve the enhancement capacity of the SiO_2@Au NPs. Compared with SERS enhancement SiO_2@Ag NPs, the existence of Au layer may be beneficial to promote the that of SiO_2@Au@Ag NPs further.

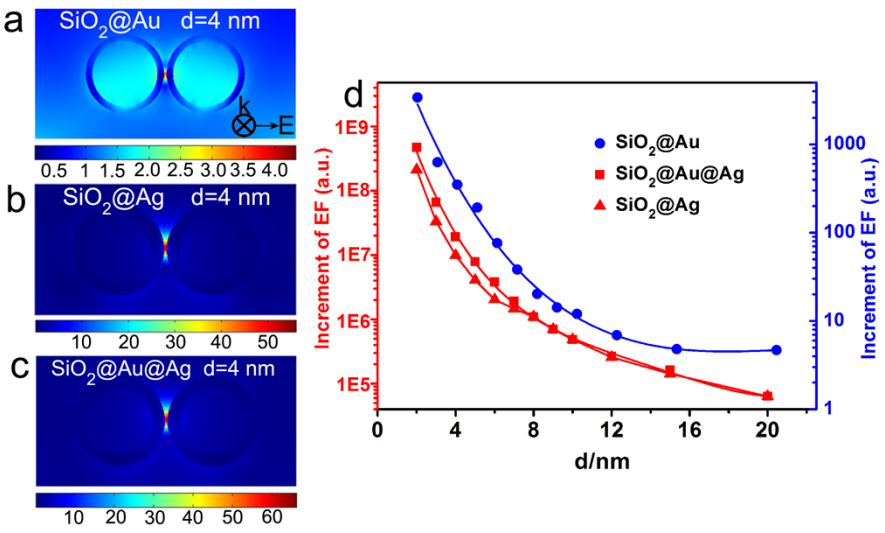

Fig. S7 Finite element method (FEM) modeling for the SiO_2@Au, SiO_2@Ag and SiO_2@Au@Ag NPs.

Part S8 SERS comparison between SiO2@Au@Ag@CD NPs and SiO2@Ag@CD NPs

As for the experimental comparison, we fabricated both SiO2@Au@Ag@CD NPs and SiO2@Ag@CD NPs and tested the SERS activity using R6G. The 10*10 μm^2 mappings on SiO2@Au@Ag@CD NPs and SiO2@Ag@CD NPs substrates were recorded under the same condition (Ex:532 nm, 10-6M R6G, acquisition time: 1s) . And the corresponding SERS spectra are then averaged and shown in the following figure (Fig.2). The SERS intensity of R6G on the SiO2@Au@Ag@CD NPs substrate is about 2-3 times of that on the SiO2@Ag@CD NPs substrate.

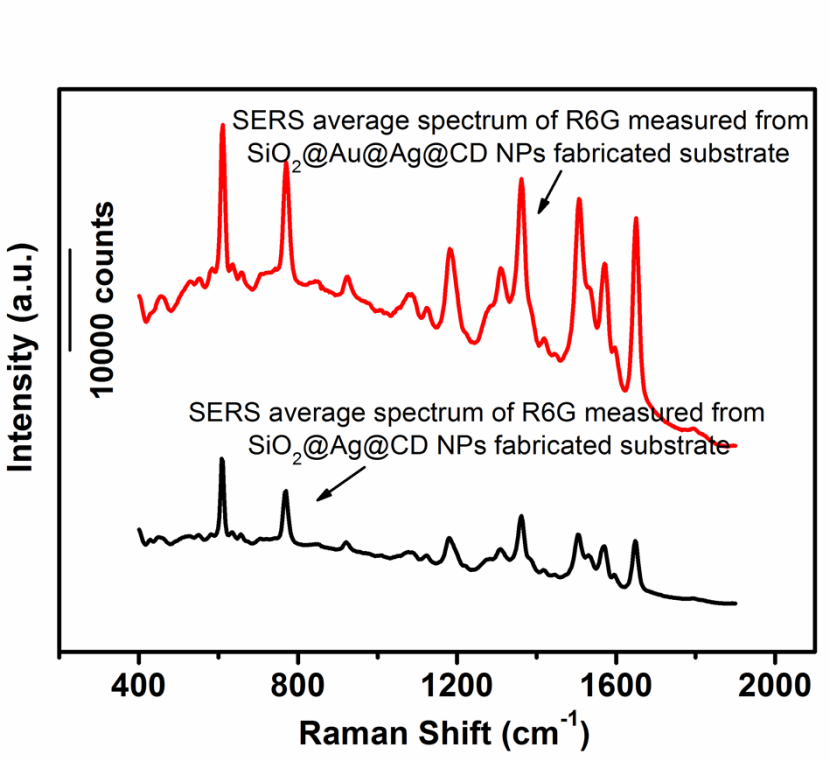

Fig. S8 Averaged SERS spectra of R6G measured from SiO2@Au@Ag@CD NPs and SiO2@Ag@CD NPs substrates, respectively. The former gives out larger SERS signals than the latter.

Part S9. Computation of some relevant vibrational modes for PCBs and PCB-CD host-guest inclusion complexes

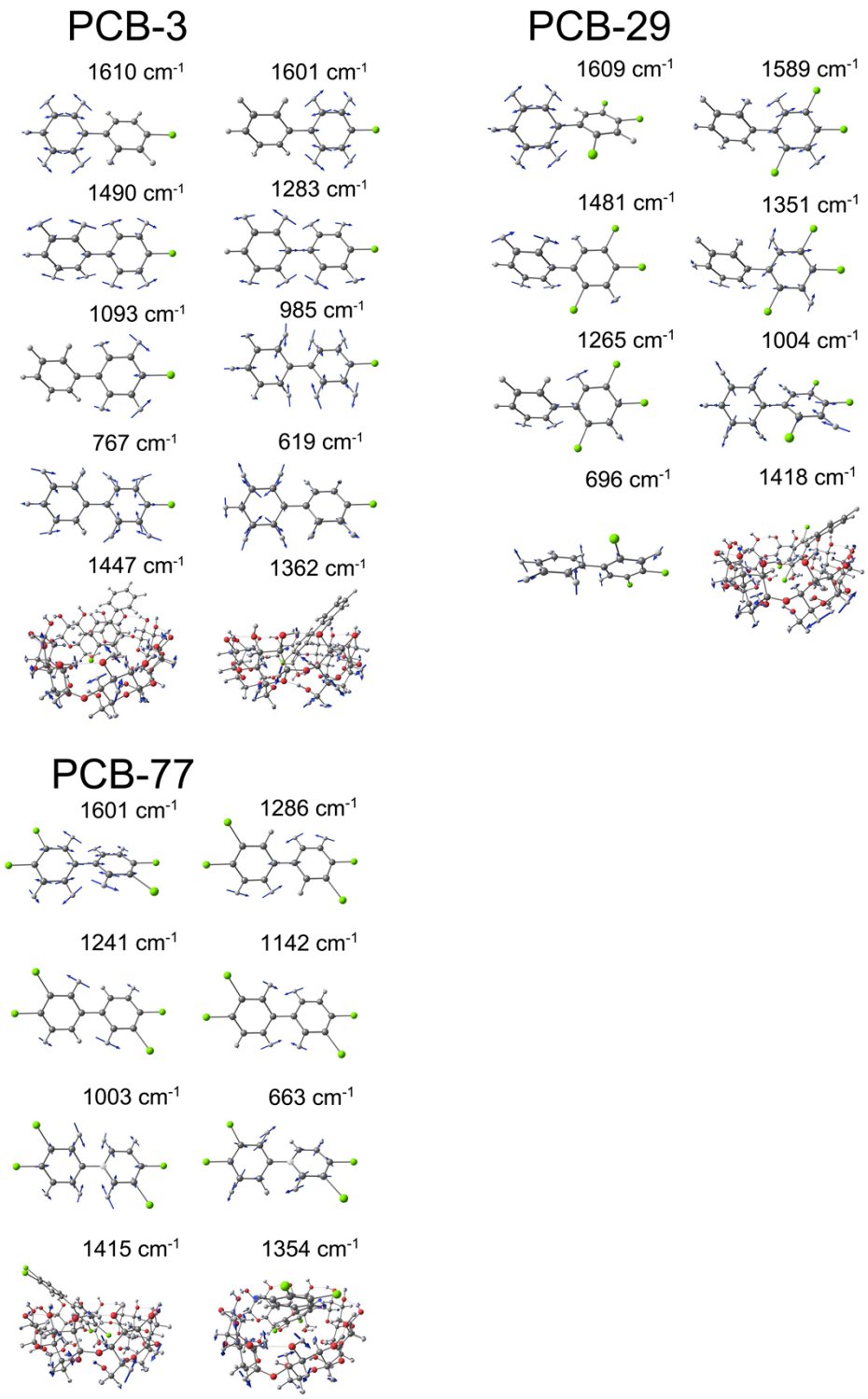

Fig. S9 Vibrational modes for PCBs and vibrational modes for PCB-β-CD host-guest inclusion complexes which can be detectable and recognized in the SERS measurements.

Part S10. SERS spectra from the blank SiO_2@Au@Ag@CD substrates and the β-CD solid powder sample

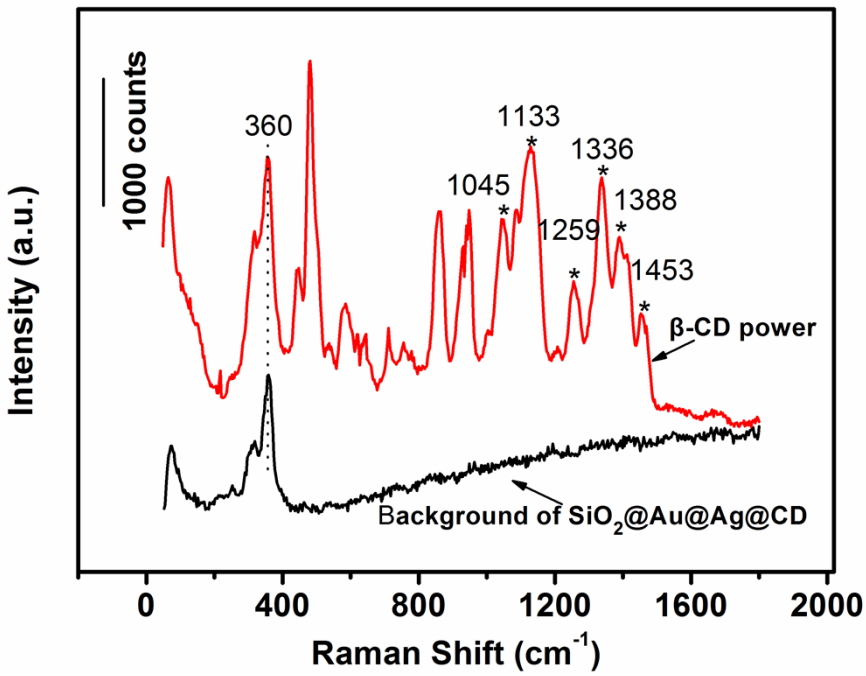

Fig. S10 SERS signals from the blank SiO_2@Au@Ag@CD SERS substrates (black) and pure β-CD solid powder sample (red).

References:

1 I. Shown, M. Ujihara, T. Imae, *J. Colloid Interface Sci.*, 2010, **352**, 232-237.

2 I. Bratu, S. Astilean, C. Ionesc, E. Indrea, J. P. Huvenne, P. Legrand, *Spectrochim. Acta Part A*, 1998, **54**, 191-196.

3 S. E. Hunyadi and C. J. Murphy, *J. Mater. Chem.*, 2006, **16**, 3929-3935.

4 P.Hildebrandt and M. Stockburger, *J.Phys. Chem.*, 1984, **88**, 5939-5944.

5 Y. Hu, Y. Shi, H. Jiang, G. Huang, and C. Li, *ACS Appl. Mater. Interfaces*, 2013, **5**, 10643-10649.

6 P. B. Johnson and R. W. Christy, *Phys. Rev. B*, 1972, **6**, 4370-4379.

7 Y. Sun, K. Liu, J. Miao, Z. Wang, B. Tian, L. Zhang, Q. Li, S. Fan, K. Jiang, *Nano Lett.*, 2010, **10**, 1747-1753.